INVERSION OF EDDY CURRENT DATA FOR CONDUCTIVE FILMS AND COATINGS THICKNESS AND CONDUCTIVITY MEASUREMENT

B. de Halleux and A. Ptchelintsev
Mechanical Engineering Department
Catholic University of Louvain
Belgium, B-1348

INTRODUCTION

Eddy current testing is currently used to determine the physical characteristics of a conductive specimen and to detect defects by measurements of electrical impedance of an eddy current probe. In this study we developed two systems of coils allowing to determine properties of conductive coatings and foils. A probe contained two plane rectangular coils connected in series and separated by a fixed distance. A coated plate or a foil was placed between the coils and the coil impedance was measured using a digital impedancemeter. The discussed probe had a large length-to-width ratio and was modeled using the simple two-conductor line model, which express solutions in terms of the integrals containing no Bessel but, only common trigonometric functions, which considerably reduces the inversion time. The method allows reproducible measurements on coated conductive sheets. Aluminum 15-45 μm layers have been measured on steel and stainless steel substrates.

THEORETICAL BACKGROUND

Let us consider a system of two rectangular δ-function coils, one of them being an induction coil and the other a pick-up coil. The geometry of the problem is shown in Figure 1. The system is placed above a coated conductive half-space. Liftoffs of these coils are equal. The induction coil length and width are respectively $2x_0$ and $2y_0$. Those of the pick-up coil are respectively $2x_1$ and $2y_1$. Electrical and magnetic properties of the coating layer are $\mu_0\mu_3,\sigma_3$ and those of the half-space are $\mu_0\mu_4,\sigma_4$. The coating thickness is m. All media are isotropic and homogeneous.

The differential equation for the vector potential $A(x,y,z)$ in an isotropic, linear and homogeneous medium due to an applied sinusoidal current density $i = i_0 e^{j\omega t}$ is

$$\nabla^2 A - j\mu\omega\sigma A + \mu i_0 = 0 \qquad (1)$$

Review of Progress in Quantitative Nondestructive Evaluation, Vol. 16
Edited by D.O. Thompson and D.E. Chimenti, Plenum Press, New York, 1997

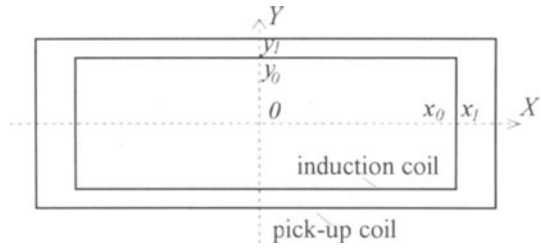

Figure 1. Eddy-current probe containing rectangular coils.

Applying to $A(x,y,z)$ the following two-dimensional Fourier transform $\overline{A}(\alpha,\beta,z)=\int_{-\infty}^{\infty}\int_{-\infty}^{\infty}A(x,y,z)e^{j\alpha x}e^{j\beta y}dxdy$, we obtain for the transformed vector potential $\overline{A}(\alpha,\beta,z)$ in the kth region the following equation

$$\frac{\partial^2\overline{A}}{\partial z^2}-\eta_k^2\overline{A}=0\,, \tag{2}$$

where $\eta_k^2=\alpha^2+\beta^2+j\omega\mu_k\sigma_k$. The general solution of the last equation is $\overline{A}^{(k)}(\eta,z)=C_k(\eta)e^{\eta_k z}+D_k(\eta)e^{-\eta_k z}$, where C_k and D_k are constants. The expressions for the vector potential $A^{(k)}(x,y,z)$ can be found by the inverse Fourier transform. The transformed vector potential $A^{(k)}(\alpha,\beta,z)$ has x and y components. The transformed boundary conditions are :

$$\overline{A}_x{}^{(k)}(\eta,l_k)=\overline{A}_x{}^{(k+1)}(\eta,l_k)\,, \tag{3}$$

$$\frac{\partial\overline{A}_x{}^{(k)}(\eta,z)}{\mu_k\,\partial z}\Big|_{z=l_k}=\frac{\partial\overline{A}_x{}^{(k+1)}(\eta,z)}{\mu_{k+1}\,\partial z}\Big|_{z=l_k}-\int_{-\infty}^{\infty}\int_{-\infty}^{\infty}I_x e^{j\alpha x}e^{j\beta y}dxdy\,, \tag{4}$$

$$\overline{A}_y{}^{(k)}(\eta,l_k)=\overline{A}_y{}^{(k+1)}(\eta,l_k)\,, \tag{5}$$

$$\frac{\partial\overline{A}_y{}^{(k)}(\eta,z)}{\mu_k\,\partial z}\Big|_{z=l_k}=\frac{\partial\overline{A}_y{}^{(k+1)}(\eta,z)}{\mu_{k+1}\,\partial z}\Big|_{z=l_k}-\int_{0}^{\infty}\int_{0}^{\infty}I_y e^{j\alpha x}e^{j\beta y}dxdy\,, \tag{6}$$

where $\eta^2=\alpha^2+\beta^2$, l_k is the z-coordinate of the boundary surface between the kth and $k+1$th regions and I_x and I_y ($|I_x|=|I_y|=I$) are x and y components of the induction current. We must take $C_1(\eta)=0$ and $B_4(\eta)=0$, where z goes to infinity. Evaluating the last terms in (4) and (6) gives

$$\int_{-\infty}^{\infty}\int_{-\infty}^{\infty}I_x e^{j\alpha x}e^{j\beta y}dxdy=\frac{4jI}{\alpha}\sin(\beta y_0)\sin(\alpha x_0)\,, \tag{7}$$

$$\int_{-\infty}^{\infty}\int_{-\infty}^{\infty}I_y e^{j\alpha x}e^{j\beta y}dxdy=\frac{4jI}{\beta}\sin(\alpha x_0)\sin(\beta y_0)\,. \tag{8}$$

Performing the Fourier inverse transform, we have for the vector potential in the first region the following expression :

$$A_x^{(I)}(x,y,z) = \frac{j\mu_0 I}{\pi}\int_{-\infty}^{\infty}\int_{-\infty}^{\infty} D\frac{\sin(\beta y_0)}{\alpha\eta}\sin(\alpha x_0)e^{j\alpha x}e^{j\beta y}e^{-\eta l-\eta z}\,d\alpha d\beta, \quad (9)$$

$$A_y^{(I)}(x,y,z) = \frac{j\mu_0 I}{\pi}\int_{-\infty}^{\infty}\int_{-\infty}^{\infty} D\frac{\sin(\beta y_0)}{\beta\eta}\sin(\alpha x_0)e^{j\alpha x}e^{j\beta y}e^{-\eta l-\eta z}\,d\alpha d\beta, \quad (10)$$

where for a magnetic conductive sheet the coefficient D is given by:

$$D = e^{2\eta l} + \frac{(\eta_3/\mu_3+\eta)(\eta_3/\mu_3-\eta)(1-\exp(2\eta_3 m))}{(\eta_3/\mu_3+\eta)^2\exp(2\eta_3 m)-(\eta_3/\mu_3-\eta)^2}. \quad (11)$$

The induced in the pick-up coil voltage is :

$$V = j\omega\left[2\int_{-y_1}^{y_1} A_y^{(I)}(x_1,y,l)\,dy + 2\int_{-x_1}^{x_1} A_x^{(I)}(x,y_1,l)\,dx\right] \quad (12)$$

$$V = \frac{4j\omega\mu_0 I}{\pi}\int_{-\infty}^{\infty}\int_{-\infty}^{\infty} D\sin(\beta y_1)\sin(\beta y_0)\sin(\alpha x_0)\sin(\alpha x_1)\frac{\eta}{\alpha^2\beta^2}e^{-\eta l-\eta z}d\alpha d\beta, \quad (13)$$

A similar relation for a system of probes, each being a two-conductor line, is given as:

$$V = \frac{j\omega\mu_0 I}{\pi}\int_0^{\infty} D\frac{\sin(y_0\eta)\sin(y_1\eta)}{\eta}e^{-\eta l-\eta z}\,d\eta, \quad (14)$$

where $2y_0$ and $2y_1$ are the respective widths of the induction and pick-up two-conductor line.

A theoretical comparison between the expressions (13) and (14) in the frequency range 5-100 kHz gave discrepancies below 2 percent when the length-to-width ratio of the rectangular coil was greater than 10. In the sequel, we will use another form of the relation (14) derived for the electrical impedance of a single layer coil, which is given as follows [1] :

$$Z = \frac{j\omega\mu_0}{\pi(y_2-y_1)^2}\int_0^{\infty}\frac{(\cos(y_2\eta)-\cos(y_1\eta))^2}{\eta^3}De^{-2\eta l}\,d\eta, \quad (15)$$

where $2y_1$ and $2y_2$ are the inner and outer width of turns. The good experimental results obtained using the last formula for conductive foil thickness measurement [1] reported earlier (see Table I) encouraged further applications of the model. The main problem remains in the probe liftoff variation. If in the case of a thin foil inspection this problem can be solved by using a soft support and applying a constant load to a probe. For the thicker foils and metal sheets the lift-off influence seriously damages precision. Let us analyze two systems of probes shown in Figures 2 and 3.

A formula currently used in electrical engineering for coupled inductances is $L_{\text{total}} = L_1 + L_2 \pm 2M$, where L_i are self inductances and M is a reciprocal inductance. Similarly for the systems of coils shown in Figures 2 and 3, we obtain for the vector potential the following expression:

Table I. Experimental results of conductive foil thickness and conductivity determination at 5-50 kHz performing eddy-current data inversion with the formula (15)

Material	Frequency kHz	Conductivity* MS/m	Actual thickness μm	Estimated thickness** μm
Copper 99.97% annealed	5	57.90 - 58.21	108 ± 1	107.6 - 108.8
			162 ± 1	161.5 - 163.4
			216 ± 2	215.3 - 217.9
	10	58.19 - 58.33	108 ± 1	107.3 - 107.9
			162 ± 1	161.0 - 161.8
			216 ± 2	214.9 - 216.0
Aluminum	20	33.76 - 33.87	30 ± 0.5	29.7 - 29.9
			45 ± 0.5	44.5 - 44.8
			60 ± 1	59.0 - 59.5
	50	33.76 - 33.89	30 ± 0.5	29.6 - 29.8
			45 ± 0.5	44.2 - 44.5
			60 ± 1	58.7 - 59.2

* - determined using a foil with known thickness;
** - determined using the measured conductivity value.

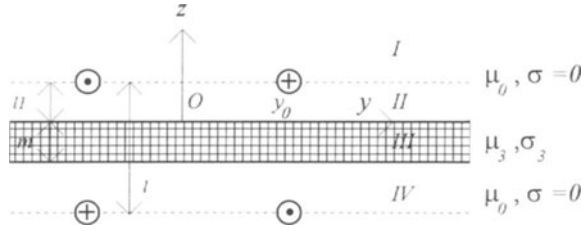

Figure 2. A conductive sheet inside coil *A*.

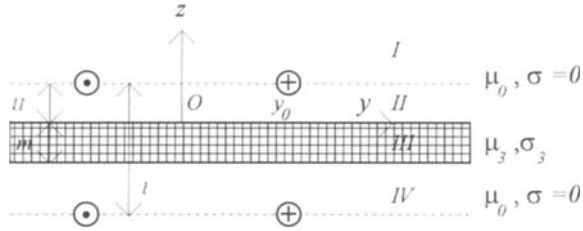

Figure 3. A conductive sheet inside coil *B*.

$$Z = \frac{j\omega\mu_0}{\pi(y_2 - y_1)^2} \int_0^\infty \frac{(\cos(y_2\eta) - \cos(y_1\eta))^2}{\eta^3} (\pm 2\mathcal{C} + \mathcal{D}e^{-2\eta l_1} + \mathcal{D}'e^{-2\eta(l-l_1-m)})d\eta, \tag{16}$$

where for a conductive sheet the $\mathcal{C}$, $\mathcal{D}$ and $\mathcal{D}'$ coefficients are given by:

$$\mathcal{C} = \frac{4\eta_3/\mu_3\eta\exp((\eta_3+\eta)m - \eta l)}{(\eta_3/\mu_3+\eta)^2\exp(2\eta_3 m) - (\eta_3/\mu_3-\eta)^2}, \tag{17}$$

$$\mathcal{D} = 1 + \frac{(\eta_3/\mu_3 + \eta)(\eta_3/\mu_3 - \eta)(1 - \exp(2\eta_3 m))}{(\eta_3/\mu_3 + \eta)^2 \exp(2\eta_3 m) - (\eta_3/\mu_3 - \eta)^2} e^{-2\eta l_1}, \quad (18)$$

$$\mathcal{D}' = 1 + \frac{(\eta_3/\mu_3 + \eta)(\eta_3/\mu_3 - \eta)(1 - \exp(2\eta_3 m))}{(\eta_3/\mu_3 + \eta)^2 \exp(2\eta_3 m) - (\eta_3/\mu_3 - \eta)^2} e^{-2\eta(l - l_1 - m)}, \quad (19)$$

with $\eta_k^2 = \eta^2 + j\omega\mu_k\sigma_k$.

To compute a multi-layered conductive sheet, the Cheng matrix method [2] was used. Results of a simulation for magnetic and non-magnetic conductive sheets using the schemes of probes shown in Figures 2 and 3 are given in Figure 5. The distance between higher and lower turns was taken to be 5 mm, the thickness of sheets 1 mm, the parameters y_1 and y_2 were respectively 5 and 15 mm, and inspected sheets were centered inside the coils.

EXPERIMENTAL SETUP AND MEASUREMENTS

All impedance measurements were taken at room temperature $20 \pm 0.5°C$ with a Hewlett Packard HP 4275A LCR-meter driven by a 486-DX4 100 MHz PC. Two probes were manufactured, whose actual dimensions and electrical properties are given in Table II. The coils were connected to the digital bridge via a one meter length cable.

To calibrate the probes, i.e. to determine an equivalent distance between the coils, a 1 mm aluminum sheet was used. Electrical impedance measurements were performed at 2 frequencies on ferromagnetic and non-ferromagnetic sheets covered on one side by a number of 15 μm aluminum foils. Varying numbers of layers modeled the coating thickness variation. Experimental results and corresponding theoretical points are given in Figure 5. The agreement between theory and experiment is good, which allows an inversion procedure based on the model (16). The agreement between experimental and theoretical points was reached using the following parameters : l=5.55 mm, l_1=2.5 mm, σ_{steel}=6 MS/m, $\sigma_{stainless\ steel}$=1.4 MS/m, $\sigma_{aluminum}$=34 MS/m. The estimated relative magnetic permeability values were 100 and 130 for coils *A* and *B* respectively. This difference can be explained by the fact that magnetic fields in these cases have different orientation and pattern.

Apparently, an inversion of eddy-current data in the case of a non-ferromagnetic sheet covered with a non-ferromagnetic conductive layer is feasible using well known inversion methods. Taking into account that with a thin coating one can infer the thickness-conductivity product [3], we need to know the coating conductivity to determine the thickness but the measurement can be limited to a single frequency, which reduces the inversion time. Results of the inversion for steel and stainless steel 1 mm plates covered with varying numbers of aluminum foils are given in Table III. The inversion was carried out via the two-variable Newton-Raphson method. Inferred thicknesses are very close to actual values for stainless steel sheets.

When inspecting ferromagnetic coated sheets, precision falls off especially at high frequency. This is caused by non-uniformity of the magnetic permeability over the space and frequency domain, a problem which can be solved if the magnetic permeability variation curves are more or less perpendicular to those of the thickness variation. This question now being extensively studied.

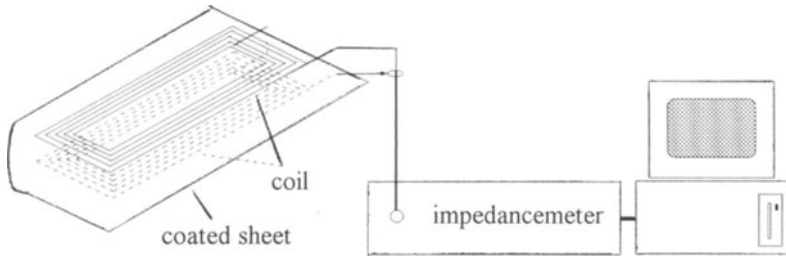

Figure 4. A schematic view of the coil and experimental setup.

Table II. Coil and measurement parameters

Parameter		Coil *A*	Coil *B*
Half width, y_1	mm	5	5
Half width, y_2	mm	15	15
Connection type		Figure 2	Figure 3
Air gap, l	mm	5	5
Resistance in air	ohm	65	65
Inductance in air	μH	109	297
Resonant frequency	MHz	8	6

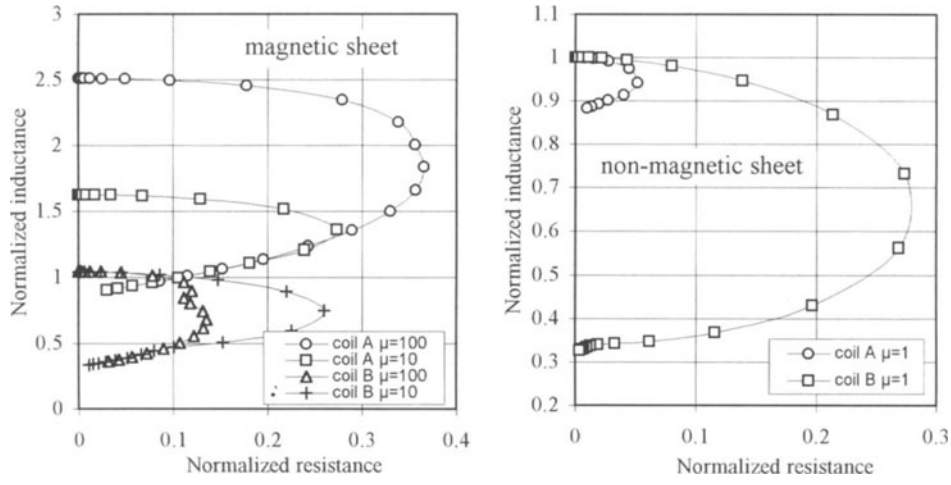

Figure 5. Theoretical normalized impedance curves for 1 mm magnetic and non-magnetic conductive sheet.

Note that coil A has a very similar behavior to that of a long cylindrical coil with a conductive rod inside, i.e. when the quantity $y_2 - y_1$ is about 10 times larger than the air-gap l, the probe becomes almost insensitive to the conductive sheet vertical displacement and tilt. When inspecting at low frequency an object with an important relative magnetic permeability μ_r the probe normalized inductance is proportional to μ_r and for $y_2 - y_1 > 10l$ it is very close to μ_r, which considerably raises sensitivity for ferromagnetic materials.

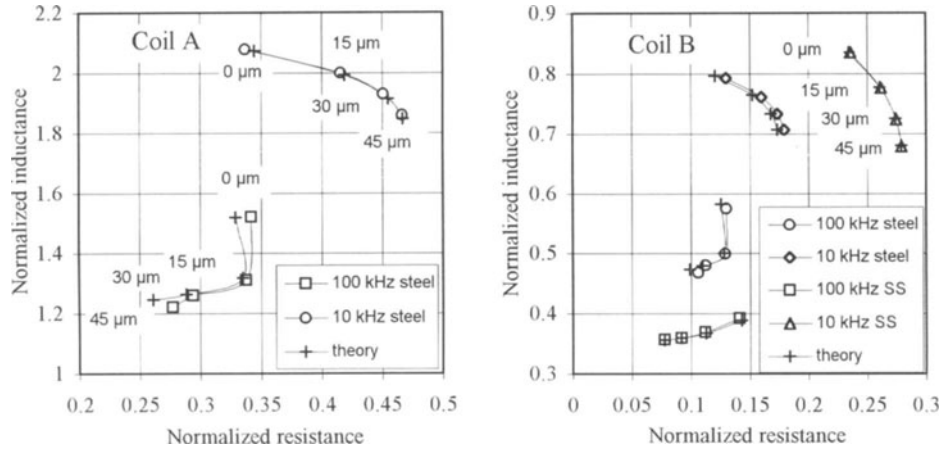

Figure 6. Experimental and theoretical points related to 1 mm steel and stainless steel sheets coated by 0, 15, 30 and 45 μm aluminum layer.

Table III. Results of eddy-current data inversion for 1 mm steel and stainless steel sheets covered by aluminum foils

Actual thickness, μm	Estimated thickness, μm	
	steel covered by Al (coil *A* 10 kHz)	SS covered by Al (coil *B* 100 kHz)
15 ± 0.5	14.7-15.0	15.8-16.0
30 ± 0.5	27.4-27.8	29.9 30.1
45 ± 1	40.5-40.9	46.0-46.2

CONCLUSION

Two systems of eddy-current probes were theoretically and experimentally studied. Both have a very small sensitivity to vertical displacements of an inspected object inside the probes, which allows reproducible eddy current measurements on coated plates. For non-magnetic plates coated on one side with a non-magnetic layer the accuracy obtained is better than 1 μm in the range of thicknesses 15-45 μm. For magnetic plates the accuracy was around 10 percent which follows from the magnetic permeability variations.

REFERENCES

1. A. Ptchelintsev and B. de Halleux, ''Two-Conductor Line Model : Rapid Inversion of Eddy Current Data for Foil Thickness and Conductivity Determination'', (to be published in Rev. Sci. Inst.)
2. C. C. Cheng, C. V. Dodd and W. E. Deeds, Int. J. NDT 3, 109 (1971).
3. J. C. Moulder, E. Uzal and J. H. Rose, Rev. Sci. Instrum. 63, 3455 (1992).